

Non-thermal photocoercivity effect in a ferromagnetic semiconductor

G. V. Astakhov^{1,*}, H. Hoffmann¹, V. L. Korenev², T. Kiessling¹, J. Schvittek¹,

G. M. Schott¹, C. Gould¹, W. Ossau¹, K. Brunner¹, and L. W. Molenkamp¹

¹*Physikalisches Institut (EP3), Universität Würzburg, 97074 Würzburg, Germany*

²*A.F.Ioffe Physico-Technical Institute, Russian Academy of Sciences, 194021 St.Petersburg, Russia*

(Dated: November 3, 2018)

We report a photoinduced change of the coercive field, i.e., a photocoercivity effect (PCE), under very low intensity illumination of a low-doped (Ga,Mn)As ferromagnetic semiconductor. We find a strong correlation between the PCE and the sample resistivity. Spatially resolved dynamics of the magnetization reversal rule out any role of thermal heating in the origin of this PCE, and we propose a mechanism based on the light-induced lowering of the domain wall pinning energy. The PCE is local and reversible, allowing writing and erasing of magnetic images using light.

Magneto-optical (MO) recording techniques currently attract much interest [1, 2, 3, 4, 5, 6] due to the non-volatility, low cost, and the removability of media they offer. Traditionally, the light is used to modify the strength of magnetic interaction. Because a very large number of magnetic ions is essential to achieve ferromagnetism the intensity of the light needed to be rather high. This results in heating of the recording media, regardless whether or not the thermomagnetic effect is the exploited physical mechanism. The resulting heat dissipation is an obviously undesirable side effect which leads to degradation of the recording media [7] and wastes significant resources. Here, we demonstrate a concept for MO recording which circumvents this problem by focusing our action on the de-pinning of domain walls, instead of trying to modify the magnetic interaction strength. The pinning efficiency can be very sensitive to the light even of low intensities, because the concentration of domain wall pinning centers is much lower than that of magnetic ions. Furthermore, in contrast to previous works on light assisted magnetization reversal [8], such a photoinduced change of the coercive field, i.e., a photocoercivity effect [9] (PCE), is local and reversible. This provides an approach to non-thermal, low-power MO recording.

Our experiments are performed on a prototype system in the form of a low-doped (Ga,Mn)As ferromagnetic semiconductor [10]. The sample used in this study is a 0.36- μm -thick $\text{Ga}_{1-x}\text{Mn}_x\text{As}$ layer (nominally $x \approx 0.01$), grown by low-temperature (LT) molecular beam epitaxy (MBE) [11] on a (001)-oriented GaAs substrate and LT-GaAs buffer. The sample shows partial compensation of Mn p-doping resulting in an insulating transport character at low temperatures. SQUID measurements show an average Mn concentration $x \approx 0.005$ and a Curie temperature $T_C = 25$ K. Because of the low hole density, the sample exhibits a clear perpendicular-to-plane magnetic anisotropy (PMA) at low temperatures [12].

Magnetic hysteresis loops are recorded by means of the magneto-optical Kerr effect (MOKE). The angle of the Kerr rotation θ is proportional to the perpendicular-to-plane component of the magnetization M , $\theta \propto M$. In our experiments we use a HeNe laser ($\hbar\omega = 1.96$ eV) with

intensity varying from 1 μW to 1 mW. The linearly polarized laser light, modulated at a frequency of 100 kHz by a photo-elastic modulator, is focused to a spot size of about 10 μm . The polarization of the reflected beam (θ) is detected by a balanced photodiode scheme and a lock-in amplifier. In the MO recording experiments of Figs. 1(c)-(f), a microscope objective with a numerical aperture 0.42 (providing a spatial resolution of a few microns) is utilized to focus the HeNe laser beam. The focusing lens is mounted on a piezo system with submicron resolution, allowing to record a surface scan of the magnetization profile. Where additional illumination of the sample is needed, we use a Xenon lamp, selecting the appropriate wavelength with a monochromator. This radiation is defocused to yield a 1-mm diameter spot on the sample surface. The experiments are performed in a flow cryostat allowing for temperature dependent experiments, with the sample immersed in superfluid helium for measurements done at $T = 2$ K. An external magnetic field of up to 1 kOe can be applied using an electromagnet mounted outside the cryostat.

Figure 1(a) shows a typical MOKE hysteresis loop for the (Ga,Mn)As sample, where the external magnetic field is applied perpendicular to the sample plane. It is taken with an attenuated HeNe laser beam at very low power ($P = 10$ μW). Figure 1(b) (filled circles) shows the same data after removing the linear background introduced by the cryostat windows. We find that at these low light levels, the 'dark' coercivity $H_{cd} = 525$ Oe. When the illumination power is increased to $P = 1$ mW (open circles), the coercive field of the region under illumination is reduced by about 40%, yielding a coercivity under illumination $H_{cl} = 285$ Oe. The difference between H_{cd} and H_{cl} is the PCE, and, as we will show below, it leads to the formation of a local domain of magnetization opposite to that of the bulk. The effect is reversible, i.e. when the power of the HeNe laser is reduced back to 10 μW , the 'dark' hysteresis loop is recovered.

This controlled formation of localized magnetization domains enables a complete MO recording cycle. To illustrate this, we define an area of 15 $\mu\text{m} \times 100$ μm on the sample surface to a byte, consisting of 8 side-by-side bits.

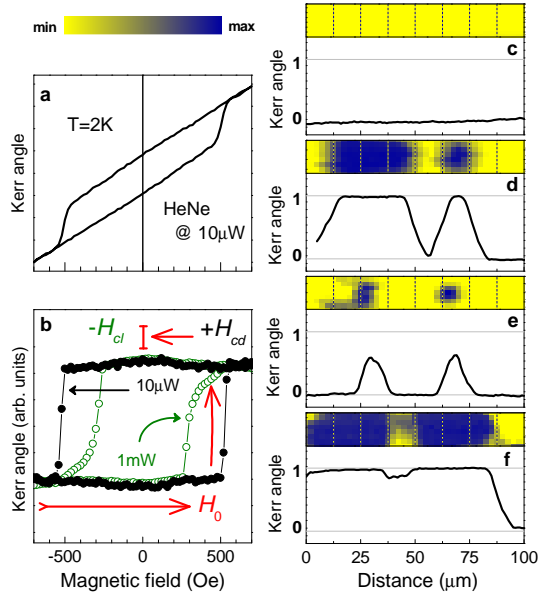


FIG. 1: (a) MOKE hysteresis loops probed by a HeNe laser. (b) MOKE hysteresis loops recorded for two powers of a HeNe laser after subtracting the linear background. Arrows indicate the light-assisted magnetization reversal process in an external magnetic field H_0 . (c) Zero-field magnetization profile obtained after initialization in a negative field (-1 kOe). Byte {00000000}. (d) as (c) but following a write procedure (performed by 1 ms pulses from a HeNe laser with $P = 100 \mu\text{W}$). Byte {01110100}. (e) as (d) following a partial deletion procedure. Byte {00100100}. (f) as (e) following a rewrite. Byte {11101110}. Thick lines in lower parts of (c)-(f) are cross sections of the magnetization profiles.

We define a bit with magnetization pointing down (up) to correspond to a logical 0 (1). The (Ga,Mn)As layer is initially prepared to be uniformly magnetized down by the application of a sufficiently strong negative magnetic field [Fig. 1(c)], yielding a {00000000} byte. A magnetic field $H_0 = +470$ Oe, which is weaker than the coercive field in the dark but stronger than the coercive field in light, $H_{cl} < H_0 < H_{cd}$ is then applied. Local illumination of the sample will now induce a transition [vertical arrow in Fig. 1(b)] into the state with magnetization directed upwards. Scanning the laser beam over the sample surface allows the writing of any desired image, which is retained even when the external field is switched off [e.g., a byte {01110100} is written in Fig. 1(d)]. In a similar manner, the data can be completely or partially erased [e.g., the byte {00100100} in Fig. 1(e)] by local illumination in a magnetic field ($H_0 = -470$ Oe) applied in the opposite direction. Missing bits can be added to a stored image at a later time [byte {11101110} in Fig. 1(f)].

Next, we address the physics of the PCE. The MOKE hysteresis loops are characterized by two key parameters: The Kerr angle in saturation (θ_s) and the coercive field H_c . These parameters can be easily extracted, respectively, from the half-height and half-width of the opening

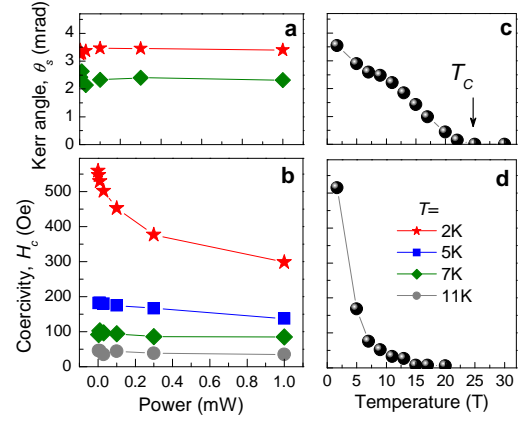


FIG. 2: Kerr angle in saturation θ_s as a function of (a) illumination power (at $T = 2$ K and $T = 7$ K) and (b) temperature (for $P = 10 \mu\text{W}$). Coercive field H_c (c) as a function of illumination power at different temperatures ($T = 2, 5, 7$ and 11 K), and (d) as a function of temperature ($P = 10 \mu\text{W}$). In all panels, the solid lines are guides to the eye.

in the hysteresis loop. Figure 2 shows the dependence of θ_s and H_c on illumination power (P) and temperature (T). The Kerr angle decreases monotonically with rising temperature [Fig. 2(c)] and is nearly independent of the illumination power [Fig. 2(a)].

Our crucial observation is the reduction of the coercive field as a function of the illumination power $H_c(P)$ as shown in Fig. 2(b). At low temperature ($T = 2$ K) the effect is rather strong with the coercivity reducing by nearly 25% before showing a saturation tendency at $P > 300 \mu\text{W}$. A photoinduced change in the coercive field, $H_{cd} - H_c(P)$, at these power levels is a rather unexpected and nontrivial behavior. The PCE disappears rapidly with increasing temperature [see Fig. 2(b)]. Note also that the coercivity 'in the dark' (i.e., recorded for $P = 10 \mu\text{W}$) also strongly depends on temperature, as shown in Fig. 2(d). To separate the two contributions, we plot in Fig. 3(a) the normalized PCE, i.e., $(H_{cd} - H_c)/H_{cd}$, as a function of temperature. Clearly, the normalized PCE decreases rapidly with rising temperature.

Interestingly, this behavior correlates with the thermal dependence of the resistance $R(T)$ of the sample obtained from a two terminal measurement between two indium contacts about 3 mm apart, and presented in Fig. 3(b). Because of the relatively low Mn concentration, the sample becomes highly resistive at low temperatures. We find that the PCE in this sample only is large when the sample is highly resistive. This may indicate that the PCE has to do with the inhomogeneous doping distribution within the layer. Such a conclusion is also consistent with control experiments we have performed on a higher doped ($x = 0.05$) perpendicularly magnetized $\text{Ga}_{1-x}\text{Mn}_x\text{As}$ layer [13]. In this high quality metallic sample, where the resistivity does not change notably in the temperature range relevant here, we have not

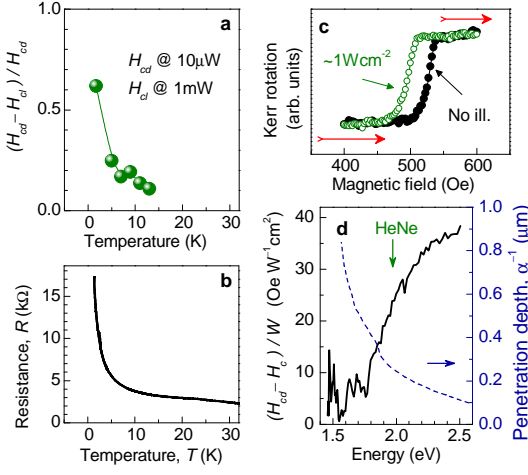


FIG. 3: (a) The light-induced change in coercive field ($H_{cd} - H_{cl}$) normalized to the coercivity in dark H_{cd} . (b) Resistance versus temperature. (c) Field-induced switching measurement with (open symbols) and without (solid symbols) additional illumination from a Xenon lamp with an intensity of about 1 W cm^{-2} . (d) Difference in coercive field scaled by the illumination intensity as function of photon energy, shown along with the characteristic penetration depth $\Lambda = \alpha^{-1}$ of the light into GaAs.

observed any decrease of the coercivity for illumination powers up to 50 mW.

To further characterize the PCE effect we have performed two-color experiments. Figure 3(c) shows field scans of the Kerr angle probed using a low power HeNe laser beam ($P = 10 \mu\text{W}$) under additional illumination from a Xenon lamp. The white-light radiation from this lamp is dispersed by a monochromator (set for a maximum intensity centered around a photon energy $\hbar\omega = 1.96 \text{ eV}$) and defocused such that the power density is of the order of $W = 1 \text{ W cm}^{-2}$. As is clearly seen in the figure, the PCE is detected even at this low power density: The difference in the coercivity with and without the illumination from the Xenon lamp is $H_{cd} - H_{c(\text{Xe})} = 25 \text{ Oe}$.

This setup allows us to record the spectral dependence of the PCE, simply by scanning the monochromator. The results of such experiments is shown in Fig. 3(d). The solid line in this figure gives the change in coercivity normalized by the illumination density W of the Xe lamp, $\frac{H_{cd} - H_{c(\text{Xe})}}{W}$. (Experimentally, we have observed that the PCE is linear with W for small W .) For energies above ca. 1.8 eV , the normalized PCE increases with photon energy $\hbar\omega$. We suggest that the spectral response mainly results from the penetration depth of the photons. For comparison, we have also plotted the penetration depth $\Lambda(\hbar\omega) = \alpha^{-1}(\hbar\omega)$ in nonmagnetic GaAs, where α is the absorption coefficient, in the same Fig. 3(d). At the highest photon energy ($\hbar\omega = 2.41 \text{ eV}$), we find $\Lambda = 0.1 \mu\text{m}$, which is two and half times shorter than the correspond-

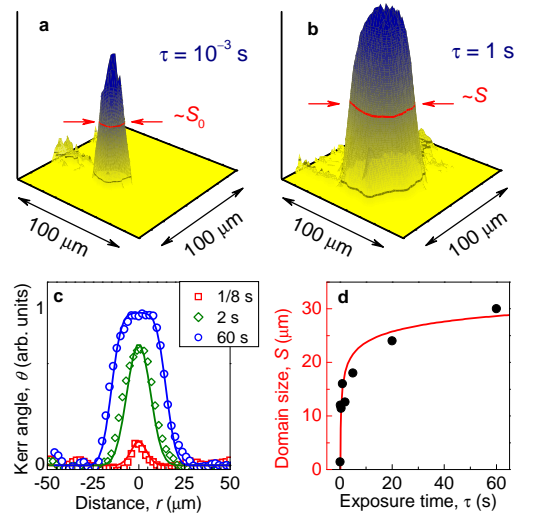


FIG. 4: The spatially-resolved dynamics of the PCE. (a) Magnetization profile of a $100 \mu\text{m} \times 100 \mu\text{m}$ area obtained after an exposure time $\tau = 10^{-3} \text{ s}$ (in a magnetic field $H_0 = 480 \text{ Oe}$) with a focused beam with $P = 500 \mu\text{W}$. (b) The same after exposure time $\tau = 1 \text{ s}$. (c) Cross sections of the magnetization profiles recorded for various exposure times in a magnetic field $H_0 = 350 \text{ Oe}$. The axis of the amplitude of the Kerr signal is calibrated such that 0 and 1 correspond to the Kerr angles obtained for the layer uniformly magnetized down- and upwards, respectively. The solid lines are fits to Eq. (1) (d) Size of the reversed domain S as a function of the exposure time τ . Solid line is a fit to Eq. (2) with $\Delta = 6 \mu\text{m}$ and $\tau_0 = 0.2 \text{ s}$.

ing Λ for photons from a HeNe laser ($\hbar\omega = 1.96 \text{ eV}$) and three times shorter than the layer thickness $d = 0.36 \mu\text{m}$. This means that the PCE occurs within the (Ga,Mn)As layer and effectively rules out any contribution to the effect arising from the substrate, the buffer layer, or the GaAs/(Ga,Mn)As interface.

Figure 4 illustrates the spatially-resolved dynamics of the PCE, with the pulse duration controlled by opening time of a mechanical shutter. The procedure is similar to the MO recording of Fig. 1: First, the sample is homogeneously magnetized in a large magnetic field (-1 kOe). Subsequently, the sample is illuminated for a time period τ by a focused light beam ($P = 500 \mu\text{W}$) in a magnetic field $H_0 = +480 \text{ Oe}$. The profile of the resulting domain of reversed magnetization is then visualized in zero magnetic field using scanning Kerr microscopy. For short illumination [$\tau = 10^{-3} \text{ s}$, Fig. 4(a)], the recorded profile is to a good approximation limited by the laser spot size, yielding $S_0 \approx 10 \mu\text{m}$. For longer exposure times, the profile widens significantly. Figure 4(c) shows linescans of the Kerr signal $\theta(r)$ through the centre of the illuminated area, characterizing the gradual increase of the size of the reversed domain with τ . In order to model these scan profiles we start from our gaussian laser spot profile $\exp(-r^2/\Delta^2)$ with $\Delta = 6 \mu\text{m}$, which is obtained from the full width at half maximum $S_0 = 2\Delta\sqrt{\ln 2}$. The

convolution of the laser spot profile with a circle of diameter S (corresponding to the size of the reversed domain) yields the Kerr signal θ as a function of distance r . For simplicity we consider the one dimensional case to be a good approximation and obtain the analytical solution

$$\theta(r) = \frac{1}{2}\theta_i \left[\operatorname{erf}\left(\frac{S/2+r}{\Delta}\right) + \operatorname{erf}\left(\frac{S/2-r}{\Delta}\right) \right]. \quad (1)$$

where $\operatorname{erf}()$ denotes the error function. Fitting to Eq. (1) as shown by solid lines in Fig. 4(c) ($\theta_i = 1$ for all curves), allows us to extract S .

In Fig. 4(d) we plot S vs. exposure time τ . The size of the reversed domain increases up to ca. $S = 30 \mu\text{m}$ for a $\tau = 60$ s exposure. One could assume this behavior to be well described in terms of a diffusion process, i.e. $S/2 \approx \sqrt{D\tau}$. However, substituting the above numbers would yield a very small diffusion constant of $D \sim 10 \mu\text{m}^2/\text{s}$. This number is in stark contrast to the low-temperature thermal conductivity of GaAs which is five orders of magnitudes larger [14, 15] and thus effectively rules out any mechanism of the PCE related to heating effects.

We are now in a position to discuss in some more detail the mechanism leading to the PCE. With an average Mn concentration of $x \approx 0.005$, the sample is insulating at low temperatures [Fig. 3(b)]. This, combined with the fact that SQUID shows ferromagnetic behavior at low temperature implies an inhomogeneous distribution of magnetic ions and holes, creating a rather irregular potential landscape. Under illumination, the photogenerated carriers will tend to smoothen this landscape by screening effects. This may well result in a lowering of the domain wall pinning energy - and thus reduce the coercive field. This mechanism also explains the absence of the effect in the metallic control sample because in a metallic sample, any local inhomogeneity will be effectively screened out by mobile holes. The potential landscape in this sample is thus already smooth without illumination, and photoexcited carriers have no influence on domain wall pinning. This argument is also consistent with the observation that, despite a higher saturation magnetization, the metallic control sample has a ~ 3 times smaller coercivity than the Mn-doped sample with $x \approx 0.005$.

The proposed model suggests that the local magnetization switching correlates with reducing the roughness of the disorder potential below some threshold value, and hence should depend on to the number of photocarriers generated during illumination. The higher the local intensity (i.e., closer to the centre of the spot) the shorter is the exposure time required to induce such a switching. Assuming that the product of the local intensity and exposure time should be a constant, one obtains for the

lateral broadening of the remagnetization area

$$S = 2\Delta \sqrt{\ln \frac{\tau}{\tau_0}}. \quad (2)$$

This reasonably reproduces the experimental behavior of Fig. 4(d) with $\tau_0 = 0.2$ s (solid line in the figure). The physical meaning of τ_0 is the time required to optically create the smallest magnetic domain. Obviously, τ_0 should depend on the illumination power P and switching magnetic field H_0 .

Summarizing, we have demonstrated local manipulation of the coercive field in a nearly insulating (Ga,Mn)As sample by low intensity illumination and performed a complete recording cycle (i.e., initialization, writing, deleting, and rewriting) on a lateral scale of a few microns. We suggest a disorder related mechanism as the most likely cause for this PCE. This proof of concept demonstration for low power MO recording is based on focussing the action of the light on modifying the pinning centers which control domain wall movement, rather than on the tradition approach of modifying the magnetization strength.

We thank M. Sawicki from IFPAN, Poland for useful discussions and R. P. Campion, A. W. Rushforth and B. L. Gallagher at Nottingham University, U.K. for providing the high quality metallic sample used in the control experiment. This work was supported by DFG-RFBR and RSSF.

* Also at A. F. Ioffe Physico-Technical Institute, RAS, 194021 St. Petersburg, Russia;

E-mail: astakhov@physik.uni-wuerzburg.de

- [1] J. J. M. Ruigrok *et al.*, *J. Appl. Phys.* **87**, 5398 (2000).
- [2] B. Koopmans *et al.*, *Phys. Rev. Lett.* **85**, 844 (2000).
- [3] G. V. Astakhov *et al.*, *Appl. Phys. Lett.* **86**, 152506 (2005).
- [4] J. Wang *et al.*, *Phys. Rev. Lett.* **95**, 167401 (2005).
- [5] A. V. Kimel *et al.*, *Nature* **429**, 850 (2004).
- [6] A. V. Kimel *et al.*, *Nature* **435**, 655 (2005).
- [7] H. Li *et al.*, *Jap. J. Appl. Phys.* **44**, 7950 (2005).
- [8] A. Oiwa, T. Slupinski, and H. MuneKata, *Appl. Phys. Lett.* **78**, 518 (2001).
- [9] B. P. Zakharchenya and V. L. Korenev, *Phys. Uspekhi* **48**, 603 (2005).
- [10] H. Ohno, *Science* **281**, 951 (1998).
- [11] G. M. Schott, W. Faschinger, L. W. Molenkamp, *Appl. Phys. Lett.* **79**, 1807 (2001).
- [12] M. Sawicki *et al.*, *Phys. Rev. B* **70**, 245325, (2004).
- [13] K. Y. Wang *et al.*, *J. Appl. Phys.* **101**, 106101 (2007).
- [14] R. O. Carlson, G. A. Slack, and S. J. Silverman, *J. Appl. Phys.* **36**, 505 (1965).
- [15] M. Soltanolkotabi, G. L. Bennis, and R. Gupta, *J. Appl. Phys.* **85**, 794 (1999).